Current Topics in Electrochemistry
Vol. 25, 2023

Original Article

Pioneering a new era with lightweight and high-performance composite materials for use in fuel cell bipolar plates

Ahmed S. Naji[1,*], Wisam J. Khudhayer[2], Farah A. Al-Saadi[1] and Douglas J. Reid[3]

[1]Chemical Engineering Department, Faculty of Engineering, University of Babylon, Hillah 51002, Iraq; [2]Department of Energy Engineering, College of Engineering/Al-Musayab, University of Babylon, Hillah 51002, Iraq. [3]Materials and Mechanical Engineering School, WSU, 2710 Crimson Way Richland, WA 99354, USA.

ABSTRACT

This study addresses the weight and cost issues associated with polymer electrolyte membrane fuel cells (PEMFCs). The United States Department of Energy (DOE) has proposed specifications for bipolar plates to facilitate fuel cell commercialization. Our research explores the development of a polymer composite material using solution casting and recycled materials. The matrix consists of polystyrene, incorporating carbon black, graphite, and carbon nanotubes as fillers. Comparative analysis, presented in tabular form, demonstrates the superior performance of our composite material in terms of being lightweight and cost-effective when compared to existing composites. The suggested material exhibits favorable electrical conductivities, measuring 14.42 S/cm and 16.464 S/cm for in-plane and through-plane directions, respectively, along with a thermal conductivity of 0.38 W/m ^{o}C.

KEYWORDS: bipolar plate, composite materials, PEMFC, polystyrene, solution casting.

INTRODUCTION

The surge in global energy demand, fueled by population and industrial growth, has heightened reliance on fossil fuels, the primary source of CO_2 emissions and environmental concerns like global warming. In response, numerous countries, including the USA, are actively exploring clean and sustainable energy alternatives [1], with fuel cells emerging as a promising option [2]. Fuel cells function by converting chemical energy, typically from hydrogen, into electrical power.

Various fuel cell types are under research and development, including direct methanol fuel cells (DMFC) [2], direct ethanol fuel cells (DEFC) [3], solid oxide fuel cells (SOFC) [4], alkaline fuel cells (AFC) [5], and polymer electrolyte membrane fuel cells (PEMFCs) [6]. Among these, PEMFCs stand out for their broad usage in portable, stationary, and transportation settings, employing hydrogen to generate electricity [2]. However, the widespread adoption of PEMFCs for domestic use is hindered by their considerable weight and cost [7], primarily attributed to fuel cell elements, notably the bipolar plates (BPP) [8]. BPP plays a pivotal role in fuel cell operation, performing functions such as reactant distribution, heat dissipation, electron conduction, and preventing reactant-coolant mixing [9]. Despite their critical functions, BPPs constitute the heaviest and most expensive component of fuel cells [10], contributing significantly to both overall weight and cost, approximately 80% and 40%, respectively [11].

Graphite has conventionally been the predominant material used in bipolar plates (BPPs) [12], providing notable advantages such as high electrical conductivity and chemical resistance [13]. However,

*Corresponding author
ahmed.najial-alawi@uobabylon.edu.iq

the inherent brittleness of graphite introduces complexities in manufacturing processes, and upscaling plate dimensions presents new challenges, contributing to heightened fuel cell size and weight. As a result, researchers are actively exploring the possibility of using alternative materials, with metals being a prominent choice due to their excellent conductivity and smaller size [14]. Nevertheless, the corrosive nature of metals necessitates additional protective measures, including electroplating and non-corrosive metal painting, albeit at increased costs and potential size increments [13, 14]. Another avenue involves coating with a low-cost polymer [15], though this approach is less favored due to decreased conductivities resulting from the inherently low conductivity of insulation polymers.

Functionalizing multi-layer plates is another technique for manufacturing bipolar plates [16]. This approach employs three separate sub-layers of graphite, metals, and polymers, each serving a distinct function. For instance, the graphite sub-layer provides high conductivity, the metal sub-layer offers excellent mechanical properties, and the polymer sub-layer mitigates corrosion. However, the drawback of this technique lies in the substantial time required for manufacturing such multi-layer bipolar plates [16]. Another attempt to create an efficient bipolar plate involves using a polymer binder with a graphite layer. However, this plate exhibits a weak resistance to corrosion [15]. Furthermore, the polymer-bind-graphite technique utilizes thermoset polymers, chosen for their liquid state, allowing them to accept a high loading of conductive filler [7], albeit at the expense of weaker mechanical properties. Presently, conductive polymer composites (CPCs) have emerged as the preferred choice [7], utilizing the polymer as a matrix filled with conductive materials. CPCs consist of pure polymers possessing excellent mechanical properties but very low electrical conductivity (10^{-14} to 10^{-7} S/cm) [17]. However, conductivity can be enhanced through blending with conductive fillers. The literature highlights various factors influencing the electrical conductivity of CPCs, with many effects associated with fillers, such as shape, type, aspect ratio, orientation, properties, loading, dispersion, and interfacial surface forces of the contained polymer matrix [18, 19].

Polystyrene (PS), a non-polar polymer renowned for its commendable chemical and mechanical properties, holds a distinct position. As a thermoplastic, it is both recyclable and extensively employed in diverse market products. In this research, PS was selected as the material to fabricate new CPCs for use in bipolar plates. Achieving filler dispersion poses a challenge due to inherent difficulties in addressing interfacial compatibility between polystyrene and filler surfaces [18]. However, it was discovered that polymers with a low degree of crystallinity (amorphous polymers) significantly enhance interfacial adhesion between polymers and fillers, facilitating good filler dispersion within the polymer matrix [19]. This property makes polystyrene suitable for dispersing carbonic fillers. Nonetheless, the electrical and thermal conductivities of polystyrene initially register very low values at ~ 10-8 S/cm [20] and 0.13 W/m°C [21], respectively. These values do not meet the 2025 technical targets set by the US Department of Energy (DOE) for bipolar plate specifications in Polymer Electrolyte Membrane Fuel Cells (PEMFC) [22, 23], as presented in Table 1.

Blending polystyrene with conductive fillers has the potential to improve its electrical and thermal conductivities, with research indicating that varying

Table 1. The typical DOE requirements for bipolar plate.

The requirement	The Target
In plane electrical conductivity	> 100(S/cm) [8]
Through plane electrical conductivity	> 20 (S/cm) [23]
Thermal conductivity	> 10 (W/m ^{o}C) [7]
Density	1.9 (g /cm^{3}) [23]
Recyclable	[24]

the sizes of conductive fillers enhances conductivity more effectively than composites using singular fillers and sizes [25]. Additionally, research by Dweiri and Sahari [26] demonstrated that composites made by solution casting exhibit higher electrical conductivity compared to those prepared *via* melt mixing.

In this study, low-cost composites were prepared through solution casting of polystyrene, involving different filler systems of rounded sizes ranging from nano-scale to micro-scale structures. The fillers, such as multi-walled carbon nanotubes (MWCNT), artificial graphite (AG), and carbon black (CB), underwent individual scrutiny as well as assessment in ternary blends. Table 2 provides details on the properties of these fillers.

2. MATERIALS AND METHODS

2.1. Materials

The materials employed in this study are recyclable, with polystyrene derived from single-use dishes, carbon black (CB) sourced from discarded printer ink, and artificial graphite (AG) obtained from the cutting of dry-battery probes. The sole non-recycled filler is the multi-wall carbon nanotube (MWCNT), which was easily and affordably prepared using a straightforward chemical method proposed by Lee and Seo [27]. The prepared MWCNT is detailed in the following section. Notably, the testing procedure incorporates a master batch of PS-MWCNT, previously prepared through melt mixing [7]. Benzene serves as the solvent for polymer dissolution and filler suspension. Figure 1 provides an overview of the general shapes of the carbonic fillers employed in the current study.

2.2. Validation of the prepared MWCNT

To validate the chemical multi-wall carbon nanotubes (MWCNT), a comparison was conducted with conventional MWCNTs based on the in-plane electrical conductivity of their composite material (PS-MWCNT). This method was chosen for its simplicity. The validation procedure consists of two steps: The first step involves preparing a single filler master batch of PS-MWCNT with MWCNT concentrations ranging from 1% to 10%, using the solution casting method. The second step entails comparing the electrical conductivity of these master batches with the diluted master batch PS-MWCNT [28] within the same concentration range. To ensure repeatability,

Table 2. Electrical and thermal properties of the materials used.

The filler	Electrical Conductivity (S/cm)	Thermal Conductivity (W/m ^{o}C)
MWCNT	$1\times10^{7} – 1\times10^{8}$ [7]	10^{3} - 6×10^{3} [21]
AG.	4×10^{3} [7]	10^{2} - 4×10^{2} [21]
CB.	10 – 100 [7]	6 – 174 [7]
PS.	10^{-8} [20]	0.13 [21]

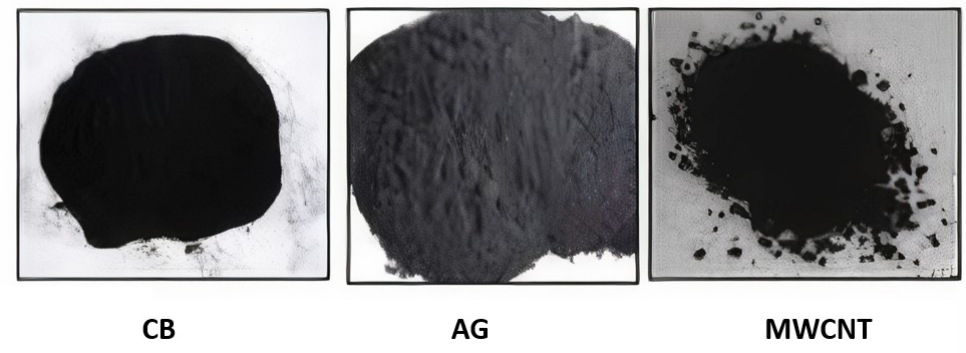

Figure 1. General shapes of the carbonic fillers.

this comparison was conducted with five samples for each loading. Table 3 presents the validation results for the prepared MWCNT.

The comparison showed a closed performance between the prepared and the diluted composites, as shown in Table 3 and Figure 2.

Figure 2 demonstrates a remarkable concurrence between the composite made with the chemical MWCNT and the diluted MWCNT, underscoring the superior performance of the chemical MWCNT. Given this favorable behavior, the chemical MWCNT was employed as a filler in the present study to formulate a cost-effective polymer composite.

2.3. Preparation of composite materials of singular and ternary filler systems

The conductive polymer composites were manufactured using solution casting followed by a compression molding procedure, as shown in Figure 3.

The manufacturing process comprises multiple stages governed by fixed operational variables, as detailed in Table 4.

To preempt any unforeseen factors that might impact the manufacturing process, such as the accumulation of filler components and reverse crystallization of the polymer, a precautionary approach was implemented. Commencing with

Table 3. Validation of the prepared chemical MWCNT.

MWCNT %	The electrical conductivity (S/cm)			MWCNT %	The electrical conductivity (S/cm)		
	PS-MWCNT diluted	PS-MWCNT Chemical	Error		PS-MWCNT diluted	PS-MWCNT Chemical	Error
1	1.20E-17	1.14E-17	6.0E-19	6	2.80E-06	2.66E-06	1.4E-07
2	2.30E-17	2.15E-17	1.5E-18	7	5.10E-06	4.95E-06	1.6E-07
3	6.40E-08	6.80E-08	-4.0E-09	8	1.52E-05	1.44E-05	7.6E-07
4	3.40E-07	3.53E-07	-1.3E-08	9	4.20E-05	3.99E-05	2.1E-06
5	6.50E-07	6.18E-07	3.25E-08	10	6.50E-05	6.58E-05	-8E-07

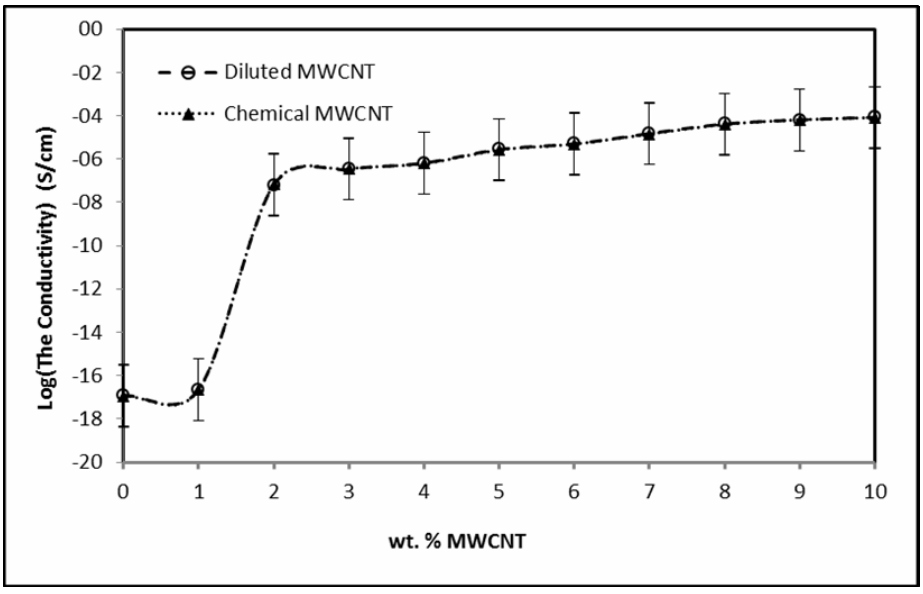

Figure 2. Comparison between the chemical and the diluted MWCNT batches.

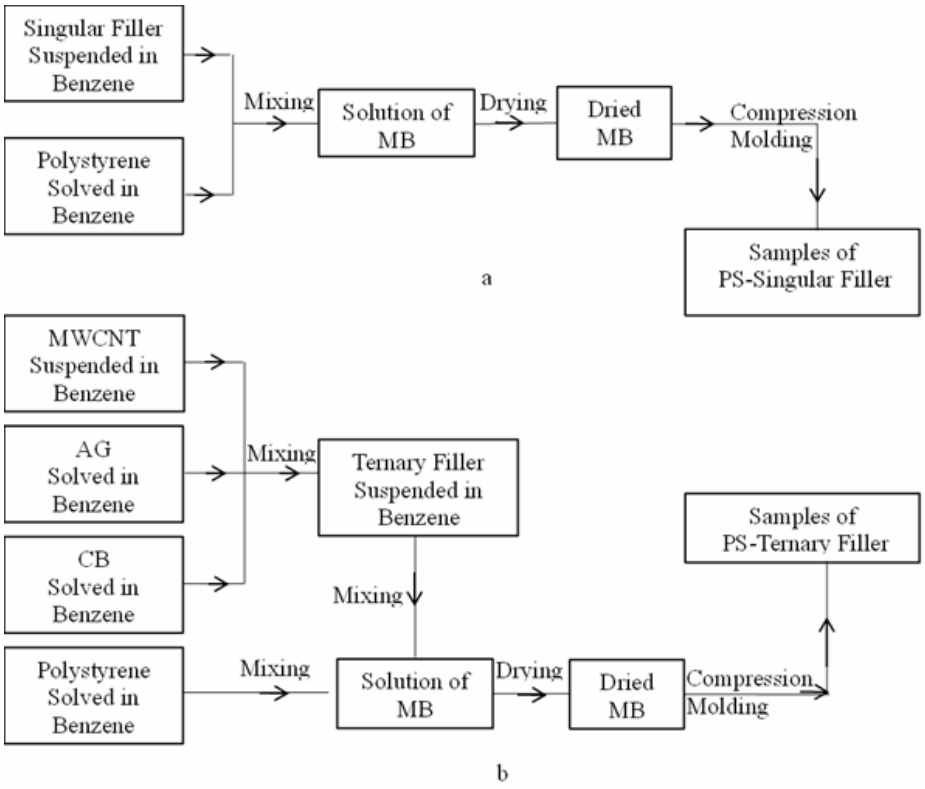

Figure 3. Preparation of the composite materials with filler system a) singular filler b) ternary filler.

Table 4. The manufacturing variables of operation.

The operation variable	The magnitude
Speed of the magnet stirrer	300 rpm
The temperature of dissolving and/or suspension	50 °C
Period of dissolving and/or suspension	15 min
The temperature of compression molding	150 °C
Period of compression molding	5 min

stage 1, the materials undergo drying in a vacuum oven at 100 °C and 80 kPa for 10 hours to eliminate any moisture that may have been absorbed during storage. Moving on to stage 2, the fillers are suspended in benzene, while the polystyrene is separately dissolved in benzene using a flask placed on a thermal magnetic stirrer. In stage 3, all the suspended filler(s) and the dissolved polystyrene are combined to produce the composite material masterbatch. Given the toxic nature of the solvent and its environmental impact, a condenser was employed to recover and recycle the evaporated solvent during casting, as illustrated in Figure 4.

Proceeding to stage 4, the composite material solution underwent 10 minutes of sonication to enhance dispersion and distribution structure [29], followed by drying in a vacuum oven to eliminate any lingering solvent residue. Advancing to stage 5, the solid batch underwent molding through hot press compression molding. For the thermal conductivity test, samples with a diameter of 1.5 cm and a thickness of 0.5 cm were prepared using compression molding. Concurrently, samples for the electrical conductivity test were fashioned in dimensions of 1.5 × 1 × 0.5 cm, as depicted in Figure 5.

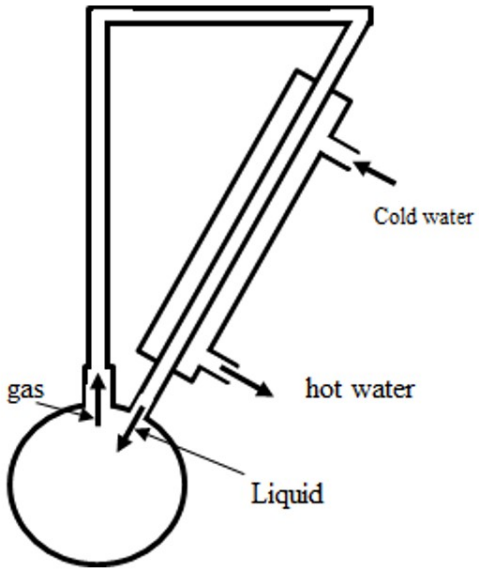

Figure 4. The solution casting apparatus with condensation.

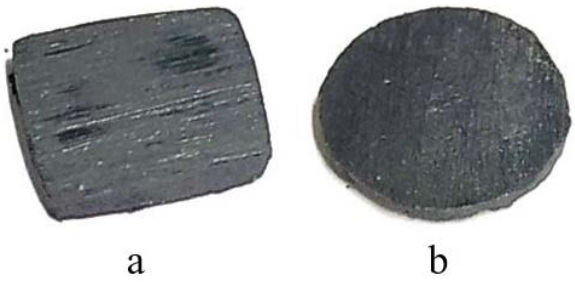

Figure 5. Prepared samples: a) for electrical test and b) for thermal test.

2.3.1. Blending systems

Heiser *et al*. [30] devised a bipolar plate crafted from a polymer composite by incorporating three distinct fillers into Nylon 6,6, both individually and subsequently in combination. Drubetski *et al*. [31] explored a polypropylene (PP) polymer composite filled separately with carbon black (CB) and carbon fiber (CF), studying the electrical conductivity effects in both cases separately and in a combined system. Mali [32] delved into various conductive fillers, illustrating the influence of singular and ternary systems on conductivity. Additionally, Yeetsorn [23] enriched PP with multiple filler systems (graphite, carbon fiber, and carbon black), investigating the effects of using diverse filler combinations. More recently, Naji [7] employed polycarbonate filled with carbon nanotubes, carbon fiber, and graphite in both singular and ternary filler systems, examining the impact of different fillers on composite conductivity. In this present work, we followed the singular and ternary approaches described above to scrutinize the influence of using singular and combined fillers on the electrical conductivity of the prepared composites.

2.3.1.1. Singular filler system

This system employs polystyrene filler with carbon nanotube, carbon black, and graphite individually denoted by codes PS-MWCNT, PS-CB, and PS-AG, as indicated in Table 5.

2.3.1.2. Ternary filler system

The preparation of the ternary filler system involves combining carbon nanotube, carbon black, and graphite simultaneously, denoted by the codes PSxG20B2NT, where 'x' represents the graphite loading. Naji (2018) [7] showed that the composition loading of the ternary filler system could improve the conductivity when combining singular filler with its threshold loading. This suggests that the makeup of the ternary system depends on the results derived from testing the individual filler composites.

2.4. Characterization

2.4.1. In-plane electrical conductivity test

A four-point probes tester ASTM D-991 was used to measure the in-plane electrical conductivity [32].

Table 5. Singular filler systems' composition.

PS%	MWCNT%	PS%	CB%	PS%	AG%
99	1	90	10	90	10
98	2	80	20	80	20
97	3	70	30	70	30
96	4	60	40	60	40
95	5	50	50	50	50
94	6	40	60	40	60
93	7				
92	8				
91	9				
90	10				

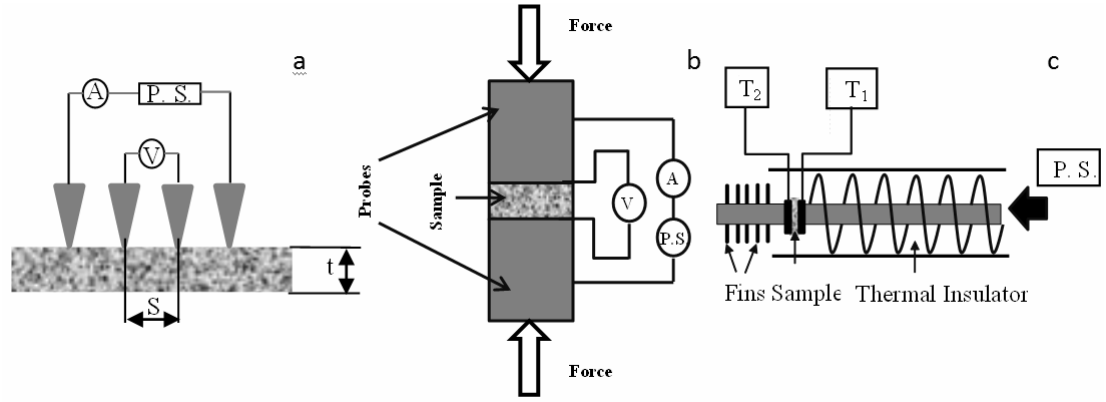

Figure 6. The testers for electrical conductivity a) In-plane, b) through-plane, and c) for thermal conductivity.

In this testing apparatus, four-point probes are arranged in a straight line.

As illustrated in Figure 6a, the inner probes are linked to a voltmeter, while the outer probes are connected in series to both a power source and an ammeter. The process for obtaining readings involves applying a specific current (I) through the power supply (PS), regulated by the ammeter. The voltmeter, connected to the inner probes, measures voltage values (V), allowing the calculation of resistance using Ohm's law. Utilizing the sample dimensions and the spacing distance between the probes, the resistivity can then be calculated [23] and [33]:

$$\rho=\frac{n\,\pi\,V}{I} \text{ and } \quad n = f(t/s) \tag{1}$$

The literature shows that the ranges of n are:

$$\begin{cases} If\ \frac{t}{S}1 \ \ then\ n = 2 \times S \\ If\ \frac{t}{S}1 \ \ then\ n = \frac{t}{ln2} \\ If\ \frac{t}{S} < 0.4 \ \ then\ n = \frac{t}{\ln\left[\frac{\sinh(t/S)}{sinh(0.5t/S)}\right]} \\ If\ \frac{t}{S} > 0.4 \ \ then\ n = \frac{Wt}{S} \end{cases} \tag{2}$$

where *t, W,* and *S* are the sample thickness, width, and spacing distance between the probes, respectively.

2.4.2 Through-plane electrical conductivity test

In this test, two copper probes are placed on either side of the sample and then compressed together between the jaws of a hydraulic press to simulate the real-world conditions experienced by a bipolar plate. As depicted in Figure 6b, a current is supplied through the power source to flow across the sample and probes, while the voltage between the probes is measured with a voltmeter. The conductivity can be determined using the following formula:

$$\sigma = \frac{I}{V} \times \frac{t}{W \times L} \tag{3}$$

where σ, *V, I*, and *L* are the sample's conductivity, voltage, current, and length, respectively. In this test, the sample surfaces should be polished first, and the surface area should be around 2.5 cm^2 while the thickness should be about 0.5cm.

2.4.3. Thermal conductivity test

In this test, a uniformly thick sample with a smooth surface is subjected to testing in the apparatus, as depicted in Figure 6c. The thermal conductivity of the sample (k) is determined using the cross-sectional area of the heated probe (A), the thickness of the sample (t), and the temperature difference recorded by the thermometer (ΔT). Thermal conductivity is calculated using the Fourier heat transfer formula:

$$k = \frac{Q}{A \times \frac{\Delta T}{t}} \tag{4}$$

The thermal conductivity test involves a power input of 50 W, a voltage ranging from 220-240 V, and a temperature range of 50-100 °C. However, specific details regarding the surface area are not provided, and the thickness of the sample must be less than 1 cm.

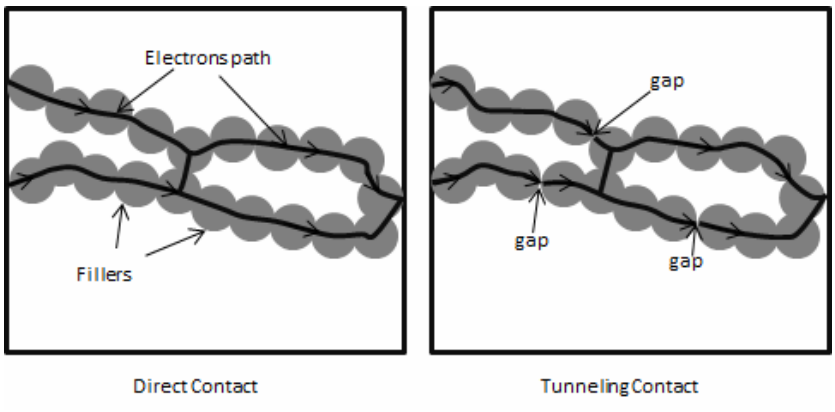

Figure 7. Electron transportation between the filler particle.

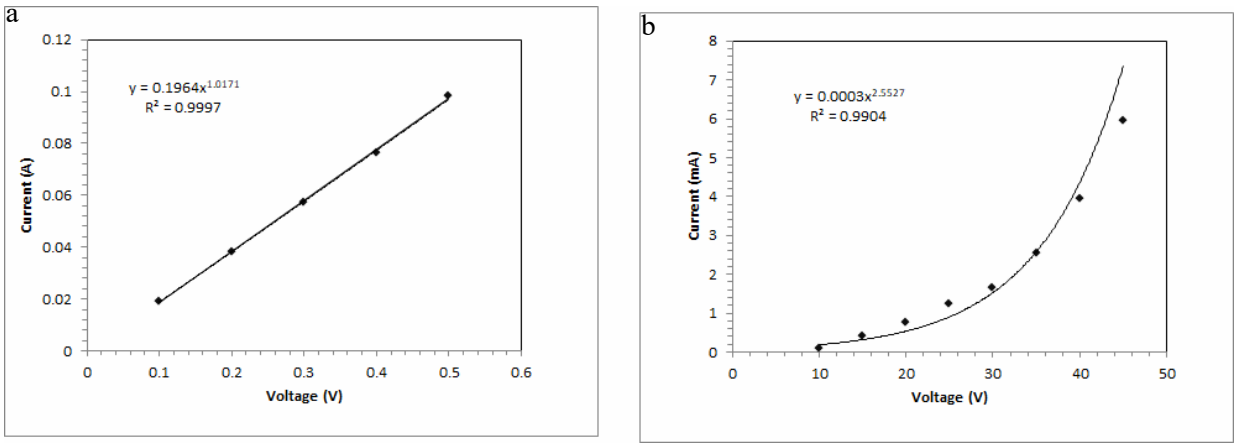

Figure 8. Direct and tunneling behaviors a) Direct Contact b) Tunneling Contact [34].

2.4.4. Morphology of the prepared samples

2.4.4.1. Scanning electron microscopy (SEM)

This analysis aims to explore the morphological characteristics of the composites. Conducted with an Ultra plus microscope (Carl Zeiss GmbH, Germany, field emission cathode) at an acceleration voltage of 3 kV, the examination involved observing cut surfaces prepared at -5 °C using a Leica microtom RM2265 with a diamond knife. Prior to observation, a 3 nm golden layer was applied as a cover to the surfaces. The resulting images offer clear insights into the distribution or agglomeration of the filler(s) within the polymer matrix.

2.4.4.2 Direct-tunneling paths

The concept of direct tunneling paths provides a direct approach to scrutinize the microstructure of the composite, especially in relation to the formation of the conductive network or electron pathways. These factors are pivotal contributors to the enhanced conductivity of the composite [34]. The two configurations illustrating these arrangements are termed Direct and Tunneling contacts of the fillers, depicted in Figure 7.

As depicted in Figure 7, electrons exhibit unhindered movement within the continuous conductive network or through direct contact, whereas electron travel requires jumping across gaps between closely packed filler particles, representing electron tunnels.

Al-Saleh *et al.* [34] demonstrated that direct contact manifests as a linear relationship between the applied current and the measured voltage (I-V) in the conductivity test. This behavior is advantageous as it mirrors the conductive properties of metals, which adhere to Ohm's law with a linear relationship

between voltage and current, as illustrated in Figure 8a.

Conversely, the non-linear (or curved) relationship signifies the electron's traversal through tunnels, contributing to reduced conductivity, as illustrated in Figure 8b.

3. RESULTS AND DISCUSSION

3.1. Electrical conductivity test

The electrical conductivity of the prepared singular and ternary filler system composites was assessed using the apparatuses depicted in Figure 6.

3.1.1. Testing of singular filler system

These composites feature polystyrene as the matrix, with carbon nanotube, carbon black, or graphite individually serving as the filler, as detailed in Table 5.

3.1.1.1. PS-MWCNT composites

Conductivity testing was conducted on polystyrene filled with multi-wall carbon nanotube (MWCNT) composites. The results, depicted in Figure 2, validate that conductivity increases with the escalating MWCNT loading, ranging from 1 wt.% to 10 wt.%. This rise in loading signifies an augmentation of electron paths within the conductive network. Figure 2 also illustrates that the threshold of the conductivity curve occurs at 2 wt.%, a crucial point considered in the subsequent blending step with the ternary filler system based on the findings of Naji [7].

3.1.1.2. PS-CB composites

Carbon black-filled polystyrene composites were also tested for conductivity, as shown in Figure 9a.

Figure 9 illustrates the incremental conductivity with an increase in carbon black loading, ranging from 10% to 60%. Notably, the conductivity curve reveals a distinct threshold at 20 wt.% CB, paving the way for the formulation of the ternary filler composite system.

3.1.1.3. PS-AG composites

The results from testing the PS-AG composite are presented in Figure 9b. The conductivity exhibits a rise with the increase in graphite content from 10 wt.% to 60 wt%. Unlike the results observed in PS-MWCNT or PS-CB, there is no evident threshold loading in the PS-AG curve. Consequently, a comprehensive range of graphite loading will be utilized in the manufacturing of ternary filler system composites, as detailed in the subsequent section.

3.1.2. Testing of ternary filler system

3.1.2.1. Electrical conductivity test

Naji [7] established that the optimal conductivity behavior in ternary filler system composites is achieved when the singular filler is incorporated at the threshold loading. Additionally, literature indicates that for bipolar plate composites, the maximum graphite loading could reach 80 wt.% in a singular filler system [8]. However, in the context of a ternary filler system, the graphite loading is typically lower, not exceeding 50 wt.% [23]. Therefore, the ternary filler system composites were formulated with a graphite loading range of 10 wt.% to 60 wt.%, while maintaining fixed loadings of 2 wt.% for MWCNT and 20 wt.% for CB, as outlined in Table 6.

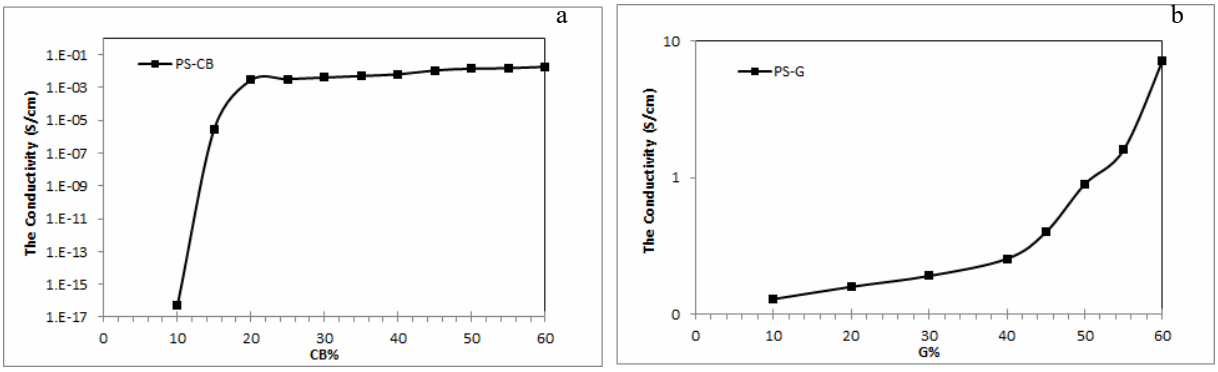

Figure 9. In-plane electrical conductivity of the composites with singular filler systems a) PS-CB and b) PS-G.

Table 6. Ternary filler system composites.

PS%	AG%	CB%	MWCNT%	Total%	The code
68	10	20	2	32	PS10G20B2NT
58	20	20	2	42	PS20G20B2NT
48	30	20	2	52	PS30G20B2NT
38	40	20	2	62	PS40G20B2NT
28	50	20	2	72	PS50G20B2NT
18	60	20	2	82	PS60G20B2NT

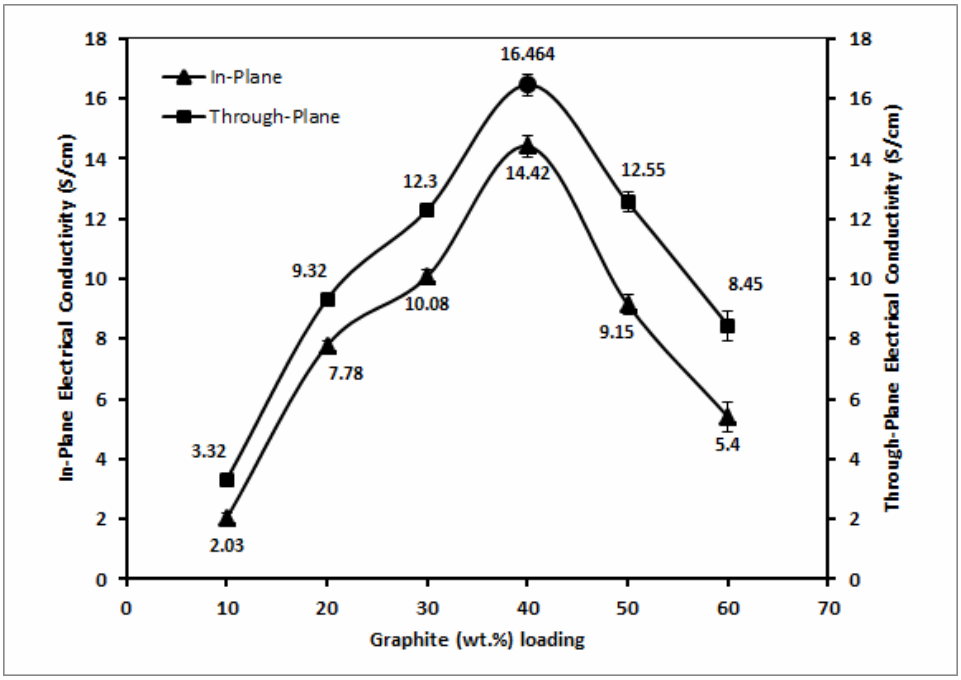

Figure 10. The effect of graphite on the in-plane and through-plane electrical conductivities of the composites of PS-filled 20 wt.% CB and 2 wt.% MWCNT.

These composites were tested for in-plane and through-plane electrical conductivities and the results are shown in Figure 10.

Figure 10 depicts the impact of graphite on the PS-2 wt. % MWCNT-20 wt. % CB composite concerning in-plane and through-plane electrical conductivities. Notably, through-plane conductivity surpasses in-plane conductivity, aligning with the findings of Naji [7].

Furthermore, Figure 10 illustrates a continuous increase in conductivity magnitudes with the augmentation of graphite loading, reaching a peak at 40 wt.%. Beyond this threshold, conductivity experiences a decline due to agglomeration. In practical terms, the nearly identical aspect ratio of graphite and carbon black particles gives rise to inadequate dispersion or agglomeration within the polymer matrix when employing a higher loading of the binary filler (a combination of graphite and carbon black) [8]. Additionally, the highest electrical conductivity magnitude at a total loading of 62 wt.% aligns with the results presented by Naji [7] and Yeetsorn [23].

The optimal electrical conductivities were achieved for the composition comprising 40 wt.% graphite,

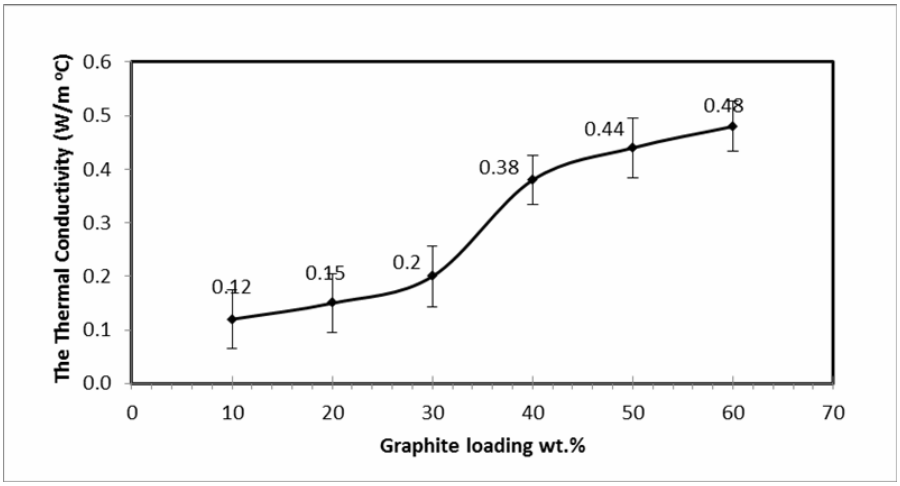

Figure 11. The impact of graphite on the thermal conductivity of composites comprising 20 wt. % CB and 2 wt. % MWCNT in PS.

20 wt.% carbon black, and 2 wt.% carbon nanotube, where the in-plane and through-plane conductivity magnitudes measure approximately 14.42 S/cm and 16.464 S/cm, respectively. This result implies that the composite displays traits reminiscent of an isotropic material, akin to metals, owing to the closely comparable magnitudes.

3.2. Thermal conductivity test

Since the target is manufacturing a bipolar plate, there is a need to test the thermal conductivity of the ternary filler system composite. Figure 11 depicts the composites outlined in Table 6.

Figure 11 illustrates the impact of incorporating graphite on the thermal conductivity of the PS composite filled with 2 wt. % MWCNT and 20 wt. % CB. Evidently, conductivity exhibits a direct correlation with the additive loading of graphite, ranging from 10 wt. % to 60 wt. %. Specifically, the thermal conductivity of the composite with a 40 wt. % graphite loading (PS40G20B2NT) is approximately 0.38 W/m ^{o}C.

3.3. Microstructure characterization results

The findings encompass SEM imaging and I-V plotting characterization curves. SEM images are presented for the composite showcasing the highest electrical conductivity (PS40G20B2NT) to illustrate filler dispersion within the polymer base. Additionally, I-V curves are depicted for composites with both the highest and lowest conductivities (PS40G20B2NT and PS10G20B2NT, respectively) to elucidate the concept of direct and tunneling contacts.

3.3.1. SEM results

The SEM images of the composite PS40G20B2NT are shown in Figure 12.

The MWCNT contributes to the network structure, enhancing electrical conductivity by establishing nano-bridges between neighboring carbonic particles, as illustrated in Figure 12a. Concurrently, the CB serves to fill the gaps between graphite particles, capitalizing on the significant size difference between CB and AG, as depicted in Figure 12b. Furthermore, these images affirm the effective dispersion of the filler within the polystyrene matrix, evident in Figure 12c.

3.3.2. Direct-tunneling contacts

The concept of direct-tunneling serves as a tool to assess the dispersion quality, determining the effectiveness of the conductive network. I-V characterization curves were generated for composites exhibiting both the highest and lowest electrical conductivities, as presented in Figure 13.

In Figure 13a, a linear relationship is observed between the applied current and the measured voltage, indicative of higher conductivity wherein electrons travel swiftly and indirectly between fillers within the network. Conversely, Figure 13b illustrates a curve-like relationship between I and V, explaining the lower conductivity.

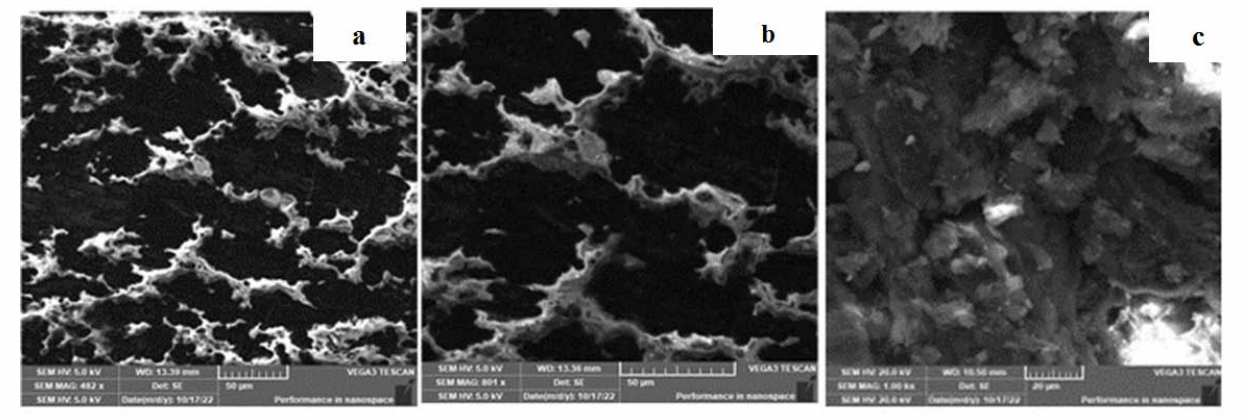

Figure 12. SEM images of the PS40G20B2NT composite.

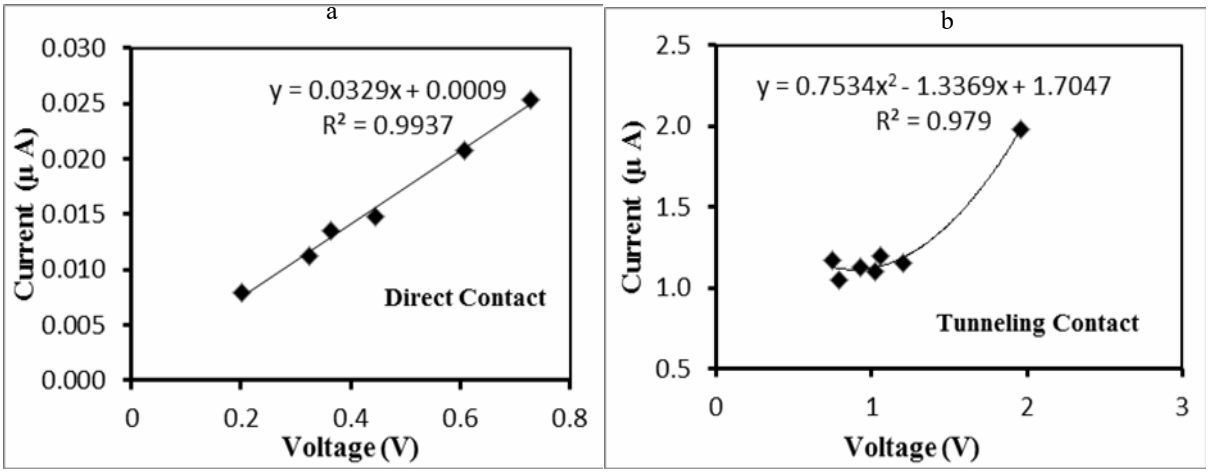

Figure 13. The behavior of a) direct contact in PS40G20B2NT and b) tunneling contact in PS10G20B2NT.

3.4. Validation of the present results

The utilization of polystyrene in the production of bipolar plates has received limited attention in the literature. Most polymers employed for this purpose include polypropylene (PP) [23] and polycarbonate (PC) [24]. For validation purposes, Table 7 provides a comparison of the current study results and the previous literature.

Table 7 compiles the outcomes of the present study alongside chosen findings from prior research, focusing on electrical and thermal conductivities, as well as density. The comparison underscores the superiority of the current material over others, even outperforming the material featured in a previous study [7].

The table reveals that the composite developed in this study is nearly as lightweight as the composites detailed in other studies, with minor discrepancies in filler loading and density. Furthermore, the composite in this study stands out for its low cost because it was manufactured from recycled materials. In terms of conductivity, the comparison indicates that the current composite exhibits superior performance in terms of both in-plane and through-plane electrical conductivities compared to others. Despite Dhakate *et al.*'s [33] composites showing higher thermal conductivity, this variance is attributed to the use of polypyrrole, a thermally unstable material [23].

Considering cost and weight, composites prepared with more economical polymers and lower filler loading are less expensive and lighter. In line with this criterion, the composite from the current work stands out as the most cost-effective and lightweight, owing to its production from recycled

Table 7. Comparison between the results of the current study and the literature.

Reference	Polymer %	Total Filler %	Thermal Conductivity (W/m ^{o}C)	Electrical Conductivity (S/cm)		Density (g/cm^3)
				In-Plane	Thro-Plane	
The Current Work	PS	62	0.38	14.42	16.47	1.28
Naji et al., [24]	PC	63	1.7	8.3	12.8	1.35
Dweiri & Sahari, [26]	PP	60	-	2.3	-	1.44
Yeetsorn [23]	PP	55	0.31	13	1.2	1.20
Mali [32]	PP	54	-	12	2.2	1.28
Dhakate et al. [33]	PP+ppy	55	0.44	9.7	0.5	1.23
DOE [22,23]	Recyclable	At least	20	100	20	1.90

polystyrene (costing just \$0.65 per kg [35], compared to other polymers priced around \$1.2 and \$2.9 per kg [17]). Additionally, there is only a marginal difference in filler loading compared to the selected works depicted in Table 7.

4. CONCLUSIONS

Considering the environment-friendly and noiseless operation of fuel cells, they have emerged as compelling alternatives for energy generation. However, the drawbacks of conventional fuel cells, notably their high weight and cost, are attributed to various factors, including the choice of materials for the bipolar plates. To address this challenge, research and development efforts are focused on identifying suitable materials, particularly those based on conductive polymer composites.

In this study, we propose a conductive polymer composite comprising polystyrene filled with 2 wt.% carbon nanotubes, 20 wt.% carbon black, and 40 wt.% graphite for the fabrication of a bipolar plate. Upon rigorous testing, the composite demonstrated notable electrical conductivities (14.42 S/cm and 16.464 S/cm for in-plane and through-plane, respectively) and thermal conductivity (0.38 W/m°C). In comparison with composites reported in the existing literature, the composite proposed in this study exhibited superior performance in terms of electrical and thermal properties, all while maintaining a low cost and nearly identical weight. These findings represent significant advancements in developing cost-efficient and high-performance bipolar plates suitable for fuel cell applications.

ACKNOWLEDGMENT

Special thanks to the University of Babylon for their invaluable support. Additionally, sincere appreciation goes to Dr. Amir Ameli from the School of Materials and Mechanical Engineering at Washington State University-Tri-Cities Campus for his support and guidance.

CONFLICT OF INTEREST STATEMENT

There are no conflicts of interest

ABBREVIATIONS

AG	:	Artificial graphite
CB	:	Carbon black
MWCNT	:	Multi-wall carbon nanotubes
CPC	:	Conductive polymer composite
DOE	:	Department of energy
PS	:	Polystyrene
PEMFC	:	Polymer electrolyte membrane fuel cells
ΔT	:	Temperature difference [^{o}C]

REFERENCES

1. Leung, P., Li, X., Ponce de León, C., Berlouis, L., Low, C. T. J. and Walsh, F. C. 2012, RSC Adv., 2(27), 10125.
2. Xing, L., Xuan, J. and Das, P. K. 2023, Chapter 2 - Fuel Cell Fundamentals, Fuel Cells for Transportation, P.K. Das, K. Jiao, Y. Wang, B. Frano, and X. Li, eds., Woodhead Publishing, 29–72.
3. Huang, J. and Faghri, A. 2014, J. Fuel Cell Sci. Technol., 11(5), 51007.

4. Kasaeian, A., Javidmehr M., Mirzaie M. R. and Fereidooni L. 2023, Applied Thermal Engineering, 224, 120117.
5. Machado, B. S., Chakraborty, N., Mamlouk, M. and Das, P. K. 2017, J. Electrochem. Energy Convers. Storage, 15(1), 11004.
6. Gautam, R. K. and Kar, K. K. 2016, Fuel Cells, 16(2), 179–192.
7. Naji, A. S. 2018, Hybrid Polymer Composite Bipolar Plates for Fuel Cell Power Plants, Washington State University.
8. Karimi, S., Fraser, N., Roberts, B. and Foulkes, F. R. 2012, Adv. Mater. Sci. Eng., 2012, 828070.
9. Yuan, X.-Z., Wang, H., Zhang, J. and Wilkinson, D. 2005, J. New Mater. Electrochem. Syst., 8, 257–267.
10. Wang, S.-H., Peng, J. and Lui, W.-B. 2006, J. Power Sources, 160(1), 485–489.
11. Planes, E., Flandin, L. and Alberola, N. 2012, Energy Procedia, 20, 311–323.
12. Petrach, E., Abu-Isa, I. and Wang, X. 2009, J. Fuel Cell Sci. Technol., 6(3).
13. Asri, N. F., Husaini, T., Sulong, A. B., Majlan, E. H. and Daud, W. R. W. 2017, Int. J. Hydrogen Energy, 42(14), 9135–9148.
14. El-Enin, S. A. A., Abdel-Salam, O. E., El-Abd, H. and Amin, A. M. 2008, J. Power Sources, 177(1), 131–136.
15. Silva, R. F. and Pozio, A. 2006, J. Fuel Cell Sci. Technol., 4(2), 116–122.
16. Heinzel, A., Mahlendorf, F. and Jansen, C. 2009, Encyclopaedia of Electrochemical Power Sources, Elsevier, 810–816.
17. Callister, W. D. and Rethwisch, D. G. 2008, Fundamentals of Materials Science and Engineering: An Integrated Approach, International Student Version, Wiley.
18. Brett, D. J. L. and Brandon, N. P. 2006, J. Fuel Cell Sci. Technol., 4(1), 29–44.
19. Fu, H., Xu, H., Liu, Y., Sun, J., Zhuang, J., Gao, X., McNally, T., Wu, D., Huang, Y., and Wan, C. 2022, Compos. Sci. Technol., 218, 109155.
20. Liao, S., Yen, C., Weng, C., Lin, Y., Ma, C., Yang, C., Tsai, M., Yen, M., Hsiao, M. and Lee, S. 2008, J. Power Sources, 185(2), 1225–1232.
21. Samsudin, S. S., Majid, M. S. A., Ridzuan, M. J. M. and Osman, A. F. 2019, Conf. Ser. Mater. Sci. Eng., 670(1), 12037.
22. Song, Y., Zhang, C., Ling, C.-Y., Han, M., Yong, R.-Y., Sun, D. and Chen, J. 2020, Int. J. Hydrogen Energy, 45(54), 29832–29847, doi: https://doi.org/10.1016/j.ijhydene.2019.07.231.
23. Yeetsorn, R. 2010, Development of Electrically Conductive Thermoplastic Composites for Bipolar Plate Application in Polymer Electrolyte Membrane Fuel Cell, Ph.D. thesis, University of Waterloo, Canada.
24. Naji, A., Krause, B., Pötschke, P. and Ameli, A. 2019, Polym. Compos., 40(8), 3189–3198. doi: https://doi.org/10.1002/pc.25169.
25. Chunhui, S. 2008, Int. J. Hydrogen Energy, 33(3), 1035–1039, doi: 10.1016/j.ijhydene. 2007.11.013.
26. Dweiri, R. and Sahari, J. 2007, J. Power Sources, 171(2), 424–432, doi: 10.1016/ j.jpowsour.2007.05.106.
27. Lee, D. and Seo, J. 2010, Accessed July 2 2023, https://arxiv.org/abs/1007.1062.
28. Ameli, A. 2018, Private Communication, WSU, USA.
29. Albozahid, M., Naji, H. Z., Alobad, Z. K., Wychowaniec, J. K. and Saiani, A. 2022, Polymers, 14(19), 4224, doi: 10.3390/polym 14194224.
30. Heiser, J. A., King, J. A., Konell, J. P. and Sutter, L. L. 2004, Adv. Polym. Technol., 23(2), 135–146, doi: https://doi.org/10.1002/ adv.20004.
31. Drubetski, M., Siegmann, A. and Narkis, M. 2005, Polym. Compos., 26(4), 454–464, doi: https://doi.org/10.1002/pc.20116.
32. Mali, T. J. 2007, Thermoplastic Composites for Polymer Electrolyte Membrane Fuel Cell Bipolar Plates, MSc thesis, University of Waterloo, Canada.
33. Dhakate, S. R., Mathur, R. B., Kakati, B. K., and Dhami, T. L. 2007, International Journal of Hydro. Energy, 32, 4537–4543.
34. Al-Saleh, M. H., Al-Anid, H. K. and Hussain, Y. A. 2013, Synth. Met., 175, 75–80, doi: 10.1016/j.synthmet.2013.05.004.
35. Made-in-china 2023, Recycled Polystyrene Granules [Online]. Available: https://www.made-in-china.com/products-search/hot-china-products/Recycled_Polystyrene_Granules.html, accessed May 2 2023.